sEMG-based Prediction of Human Lower Extremity Movements by Using a Dynamic Recurrent Neural Network

Chengkun Cui[1], Gui-Bin Bian[1], Zeng-Guang Hou[1], Xiao-Liang Xie[1], Liang Peng[1], Dongxu Zhang[1]

1. The State Key Laboratory of Management and Control for Complex Systems, Institute of Automation, Chinese Academy of Sciences, Beijing 100190, China

E-mail: {cuichengkun2014, guibin.bian, zengguang.hou, xiaoliang.xie, liang.peng, dongxu.zhang}@ia.ac.cn

Abstract: In this paper, a novel robust nonlinear model is proposed to predict human lower extremity motion based on the multi-channel surface electromyography (sEMG) signals. The prediction model is established by a data-driven dynamic recurrent neural network. The sEMG signals acquired from human lower extremity muscles are used as the inputs of the prediction model. The outputs of the model are joint angles of hip, knee and ankle. Different from the traditional feedforward network structure, this model has several feedback loops, thus it can take advantage of the output feedback information. To validate the effectiveness of the proposed method, five able-bodied people participated in the cycling exercises and relevant data were recorded in real time. The performance of the proposed prediction model is compared to those of the feedforward neural network with augmented inputs (FFNNAI) for the motion prediction accuracy and robustness. The results show that the proposed method provides acceptable performance which is clearly better than the FFNNAI-based approach under different experimental schemes.

Key Words: sEMG, motion prediction, dynamic recurrent neural networks, human-robot interaction

1 INTRODUCTION

There have been an increasing number of wearable robots in the world designed for locomotion assistance and rehabilitation over the last decades. Exoskeletons [1], active orthoses [2] and powered prostheses [3] are all typical wearable robots. As so far, existing wearable robots are still confronted with a lot of challenges on mechanical designs and control strategies. One of the major challenges is that the robot usually does not have the ability to adequately identifying the intentions and actions of the human wearer [4]. Hence, wearable robots may not accurately provide needed motion assistance for different users. Moreover, recent evidences with respect to the results of rehabilitation exercises have indicated that the motion intention plays a significant role in rehabilitation process [5]. Therefore, accurate recognition of users intentions and actions is indispensable during locomotion assistance and rehabilitation process.

Surface electromyography (sEMG) signals measured from the human muscles have been taken as one of the major human-robot interaction information sources in a lot of robot systems for its strong relationship with human motion. In recent years, there are numerous researches based on the sEMG signals for decoding human body movements (e.g. force [6], joint angle [7] and joint torque [8]). For instance, sEMG-based motion estimation techniques are widely investigated by many researchers. In [9], Song Rong et al. used a recurrent artificial neural network model to estimate voluntary elbow torque from sEMG signals and kinematic data in dynamic situations. The results indicated that sEMG signals together with kinematic data can get good performance in elbow joint torque estimation. Kwon et al. [10] investigated a feedforward neural network (FFNN) for real-time upper limb movement estimation. The network inputs are the features extracted from sEMG and the angular velocities of the elbow and shoulder, and the outputs are estimated joint angles of the elbow and shoulder. The experimental outcomes showed acceptable joints estimation performance. Ngeo et al. [11] presented an FFNN to estimate the finger joint angles using muscle activation inputs from sEMG data and got reasonable accuracies for finger movements by experiments. However, sEMG-based motion estimation techniques can only estimate the current motion intention of users. Due to this limitation, estimation methods may not response timely for the system in which the delays cannot be ignored. Unfortunately, there are some inevitable delays existing in wearable robots, such as delays in signal acquisition and processing, delays in motion control operation and so on. These delays probably have bad effects on the real-time capability and the interaction control performance of the wearable robot system.

Based on the above consideration, some researches lately proposed sEMG-based motion prediction methods to relieve the detrimental effects caused by delays. Compared with estimation approaches, the prediction methods can predict future movement intention. Therefore, motion prediction may have a better performance in compensating the delays and improving the real-time capability of the wearable robot system. It is worth to note that the distinction between motion prediction and motion estimation are not very clear in many literatures. However, by considering the problems caused by delays in the robot system, this distinction needs to be emphasized. As for movement prediction

978-1-4673-9714-8/16/$31.00

methods, Loconsole et al. [12] used feedforward neural network with augmented inputs (FFNNAI) to process the time sequence prediction problems. They established two FFNNAIs to predict the human shoulder and elbow joint torques from sEMG signals acquired from relative muscles, respectively. Both of their network models used 4 historical inputs, namely, the input delay order is 4. The torque prediction errors through experiments are acceptable. Nevertheless, this model did not use the historical output data and may get a poor outcome when users movement changes fast. Li et at. [13] built a high order recurrent neural network to approach the nonlinear relationship between the ankle joint torque and the evoked EMG signals. Then the network was used to predict the ankle joint movements. The network model used 4 historical inputs and 3 historical outputs, namely, the input delay order is 4 and the output delay order is 3. This model used the output feedback information and can get higher accuracy. However, this nonlinear relationship was just reflected in two coupling terms between the specified inputs and specified feedback outputs. Thus, this method might not reflect the complex relationship between human movements and sEMG signals well in many other different cases. Based on the above analysis, the techniques about human body motion decoding are not perfect and still have large exploration space.

A novel lower extremity movement prediction method is put forward in this paper. The performance of proposed prediction strategy is validated and compared with the FFNNAI-based method. Experiment results show a good prediction capability on lower limb joint angles prediction by using the proposed approach. Notice that this work can also apply to other types of locomotion such as force, joint torque and so forth. The remainder of the paper is organized as follows: section II introduces data acquisition and processing of the sEMG signals. The prediction model and algorithm of the lower limb joint movement are presented in Section III. The experiments and discussion of the prediction scheme are given in the Section IV. Section V gives the conclusion and future works.

2 ACQUISITION AND PROCESSING OF SEMG SIGNALS

Cycling exercise is selected as the locomotion mode in our experiments, which is one of the most common activities of daily living. In order to acquire the convincing experimental data, five healthy male subjects were recruited in the cycling exercises. The average age of the subjects is 25.5 ($\pm$1.6) years; the average height is 1.71 ($\pm$0.04) m; the average weight is 63.8 ($\pm$6.3) kg. All the subjects were asked to do the cycling exercise at their own comfortable speed, which can give them a natural feeling and may record relative stable and regular signals easily. For each subject, one motion trial lasts about 10 s. During cycling, seven channels of sEMG signals were simultaneously sampled at 2 kHz from vastus rectus muscle (VR), vastus lateralis muscle (VL), semitendinosus muscle (SM), biceps muscle of thigh (BM), tibialis anterior muscle (TA), extensor pollicis longus (EP) and gastrocnemius muscle (GM). At the same time, the three joint angles of human lower extremity were collected with the sampling rate of 100Hz. Raw seven-channel sEMG signals and three joint angles signals from one of the five able-bodied individuals is shown in Fig. 1. Moreover, the sEMG signals during maximum voluntary contraction (MVC) for each person were recorded for data normalization. The data acquisition process of sEMG signals and joint angles during cycling exercises from one subject is shown in Fig. 2. Raw sEMG signals

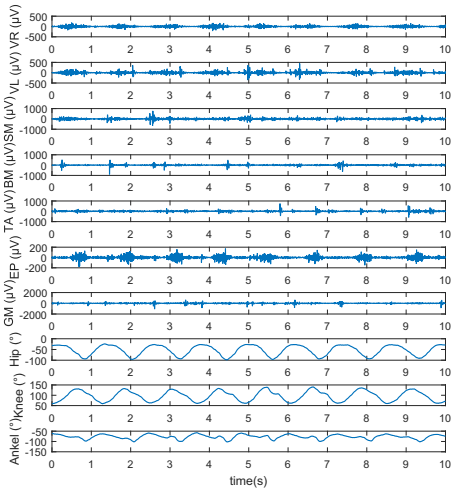

Figure 1: Raw seven-channel sEMG signals and three joint angles signals from one of the five able-bodied individuals

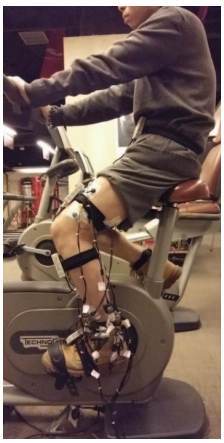

Figure 2: The data acquisition process of sEMG signals and joint angles signals during cycling exercises from one subject

are always contaminated by many noises, such as industrial frequency interference, high-frequency interference and movement artifacts. In order to remove these noise signals, a 50 Hz notch filter and a 20-500 Hz band-pass filter are applied to sEMG signals. After filtering, the multi-channel sEMG signals are full-wave rectified. This operation can be described as

$$sEMG_{rec}(t) = |sEMG(t)| \quad (1)$$

where t is the sampling point. The changing process of amplitudes of sEMG signals can be much more clearly indicated by full-wave rectification. Then, each channel of sEMG signals should be normalized by the amplitude peak values of the sEMG obtained during MVC.

$$sEMG_{norm}(t) = \frac{sEMG_{rec}(t)}{|sEMG_{MVC}|} \tag{2}$$

As sEMG signals and the joint angle signals have different sampling rates, it is necessary to implement the synchronization between them. Because the sampling frequency of sEMG (2k Hz) is 20 times higher than that of the joint angle (100 Hz). Thus, the normalized sEMG data are averaged over a sliding window of 20 samples (with no overlapping). This operation can be implemented by

$$sEMG_{ave}(k) = \frac{1}{W} \sum_{t=(k-1)W+1}^{kW} sEMG_{norm}(t) \tag{3}$$

where $sEMG_{ave}(k)$ is the average of the normalized sEMG on the sampling interval $[(k-1)W+1, kW]$ and $W = 20$. After synchronization, each channel of sEMG and each joint angle have 1,000 sample points for every trial of cycling exercise. Since human body movements perform a strong low frequency property, a fourth-order low-pass Butterworth filter with cut-of frequency 5 Hz is selected for smoothing the signals to simulate the natural filtering property of human muscle.

Although the seven-channel sEMG signals are monitored at the same time, not all the channels of sEMG have strong relevance with the lower limb movements. By considering the problems of data redundancy and computation complexity, the seven channels of sEMG signals should be selected appropriately based on the correlation with lower extremity joint angles. The correlation coefficient indicator is calculated to analyze the correlations between the lower limb joint angles and seven-channel sEMG signals. The absolute value of correlation coefficients between two random variable X, Y can be represented as

$$\rho(X,Y) = \left| \frac{Cov(X,Y)}{\sqrt{D(X)D(Y)}} \right| \tag{4}$$

where $Cov(X,Y)$ is the covariance between X and Y; $D(X)$ and $D(Y)$ are the variance of X and Y, respectively. The correlation coefficients between lower limb joint angles and seven-channel sEMG signals are shown in Fig. 3. The lateral axis denotes the seven channels of sEMG signals and the vertical axis represents the absolute value of correlation coefficients between sEMG and joint angles. From Fig. 3(a), it can be clearly see that $\rho(VR, hip)$ and $\rho(VL, hip)$ are much higher than others, which means the sEMG from VR and VL show remarkable correlation with the hip joint angle. In the same way, it can be conclude that the knee joint angle has remarkable relevance with the sEMG of VR, VL, EP and the ankle joint angle performs strong correlation with the sEMG of EP. Thus, the sEMG signals from VR, VL and EP contain a lot of useful motion information and are selected to predict human lower limb movements.

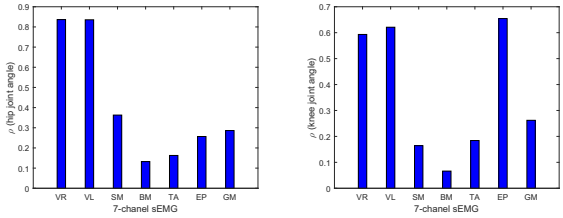

(a) Correlation coefficients between hip joint angle and seven-channel sEMG

(b) Correlation coefficients between knee joint angle and seven-channel sEMG

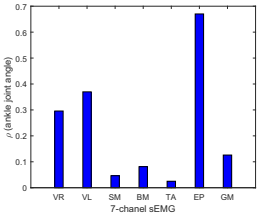

(c) Correlation coefficients between ankle joint angle and seven-channel sEMG

Figure 3: Correlation coefficients between lower limb joint angles and seven-channel sEMG

3 LOWER EXTREMITY MOVEMENT PREDICTION BASED ON A DYNAMIC RECURRENT NEURAL NETWORK

In this section, we will model the relationship between lower extremity joint angles and the selected sEMG signals. The inputs of the prediction model are the sEMG signals from VR, VL and EP selected from correlation analysis. The outputs are joint angles of hip, knee and ankle, which can be considered as the outward manifestation of human lower limb movements.

Consider the relationship between the sEMG and joint angles as the following nonlinear autoregressive model with external inputs (NARX):

$$\begin{aligned} \theta(t) = f(&u(t-1), \cdots, u(t-M), \cdots \\ &\theta(t-1), \cdots, \theta(t-N)) \end{aligned} \tag{5}$$

where θ is the joint angle vector; u is the amplitude vector of the sEMG; M is the order of input delays; N is the order of feedback delays and t is the sampling point. For more precise modeling, an NARX-type dynamic recurrent neural network (NARX-DRNN) is built for nonlinear approximation. The schematic diagram of the NARX-DRNN is shown in Fig. 4. Notice that the number of model inputs and outputs can be regulated by actual demands. In this paper, the number of network outputs is three and the number of inputs is due to the delay orders. The hyperbolic tangent function and linear function of our NARX-DRNN are selected as the activation functions of the hidden layer and output layer, respectively. Therefore, the proposed model can be denoted as follows:

$$\hat{\theta}(t) = W_{out}[\frac{2}{1+e^{-2(W_{in}p+b_{in})}} - 1] + b_{out} \tag{6}$$

where $\hat{\theta}$ is the prediction of the joint angle vector at every

time step; p is the input vector and it can be represented as $p = [u(t-1), \cdots, u(t-m), \hat{\theta}(t-1), \cdots \hat{\theta}(t-n)]$; W_{in} and W_{out} are the weight matrices of the hidden layer and output layer; b_{in} and b_{out} are the threshold vectors of the hidden layer and output layer. As the network has several feedback loops, it can use the historical output data effectively. Compared with [13], all the inputs and feedback outputs of this model are contained in the nonlinear relationship between the sEMG and movements. Hence, this model might be more general to decode the relationship between human body motion and sEMG signals in different cases. For simplicity, the input delay order and the output delay order for our network are set to the same in this paper. Thus, we will only give the input delay order in the subsequent parts. The proposed model is trained by the Bayesian regularization algorithm which can guarantee its prediction accuracy and generation ability.

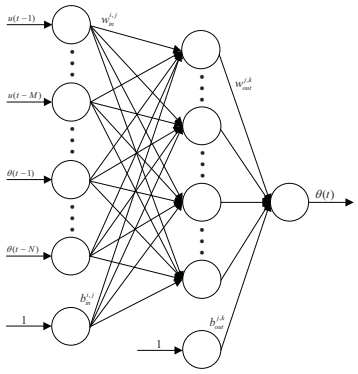

Figure 4: The schematic diagram of the NARX-DRNN

4 EXPERIMENTS AND DISCUSSION

In this section, two different experimental schemes are designed to validate the effectiveness of our NARX-DRNN model. One is the subject-dependent experiment, in which the data of one subject's cycling exercise is divided into training set and testing set by some points of time. Since the cycling motion for one subject lasts 10 s, the first 7 s data are used to train the network and the remaining 3s data are selected for testing in this section. This subject-dependent experiment has been applied to one specific subject's movement data by random selecting. The other is the subject-independent experiment that uses more data from different people for training and testing. For instance, Among the five subjects' exercise data, four people's data are randomly chosen as the training set and the rest one is used as the testing set. The random selection method mentioned above needs to be conducted a certain number of times to ensure the credibility of the experiment results. At the same time, the contrast experiments are carried out to compare the performance of the proposed NARX-DRNN and the traditional FFNNAI. For fair comparison, the prediction accuracy under the same network complexity is selected as an indicator. It is because the real-time performance of the algorithm mainly depends on the network complexity. When neural networks are used for prediction of time sequence, the hidden layer structure and input delay order are significant parameters of the network complexity. The hidden layer structure parameters consist of the number of hidden layer and the number of hidden layer nodes. In order to reduce the computation time and the complexity of the network, we set the number of hidden layer as one and select the nodes and input delay order as small as possible. In order to measure the prediction accuracy, the root

Table 1: Results of the subject-dependent experiment

Joint Angle (°)	RMSE (NARX-DRNN)	RMSE (FFNNAI)
Hip	3.4253	7.3834
Knee	4.1185	8.3920
Ankle	3.1341	6.8144
Mean	3.5593	7.5300

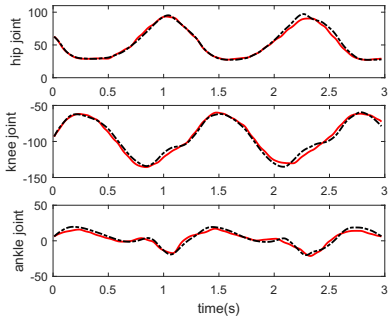

(a) Performance of NARX-DRNN in the subject-dependent experiment

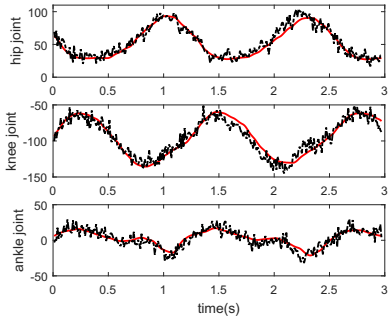

(b) Performance of FFNNAI in the subject-dependent experiment

Figure 5: Comparison of the joint angle prediction performance by using NARX-DRNN and FFNNAI in the subject-dependent experiment

mean square error (RMSE) is selected as the evaluating indicator, which can be defined as

$$RMSE = \sqrt{\frac{1}{T}\sum_{t=1}^{T}(\hat{\theta}(t) - \theta(t))^2} \tag{7}$$

where T is the size of the test sample; $\hat{\theta}$ is the predicted joint angle; θ is the measured one. By considering the effects of random initialization of network weights, the final result of each experiment is obtained by calculating the average of five execution results in a row.

In Fig. 5 and Fig. 6, the red line denotes the actual joint angles measured by the angle sensor and the black line represents the estimated results. For the subject-dependent experiment, the number of the hidden layer nodes and input delay order are 10 and 2, respectively. Table 1 and Fig. 5 compare the prediction performance of joint angles by using NARX-DRNN and FFNNAI, respectively. As it can be seen from the results, the RMSE for every joint angle by using NARX-DRNN is less than 4° which is clearly lower than those of FFNNAI. For the subject-independent experiment, since the experimental data are larger, the number of the hidden layer nodes and input delay order are increased to 20 and 3, respectively. The comparison results are given in Table 2 and Fig. 6. It can be seen that each RMSE of NARX-DRNN is less than 5° which shows an acceptable outcome for the motion data recorded from different persons. In contrast, the performance of FFNNAI is obviously unable to meet the requirement. Thus, the NARX-DRNN is less sensitive to different people's data, which means NARX-DRNN has better robust performance and generalization ability for different people. Based on

Table 2: Results of the subject-independent experiment

Joint Angle (°)	RMSE (NARX-DRNN)	RMSE (FFNNAI)
Hip	4.2558	8.9634
Knee	4.3756	10.3874
Ankle	3.5693	7.9670
Mean	4.0669	9.1060

the above analysis, the proposed NARX-DRNN can be applied to both one person's motion data and several different persons' motion data. Furthermore, the average RMSE of NARX-DRNN is smaller than 5° for two different experimental schemes. Therefore, we can safely draw a conclusion that the prediction performance of NARX-DRNN shows good performance both in prediction accuracy and in robustness. In addition, the performance of the proposed NARX-DRNN is much better than that of FFNNAI which can be seen from the compared experiments. Last but not least, the response time of NARX-DRNN is about 10.4 ms (containing sampling time) for predicting the joint angles of every sampling time, which is an acceptable delay for a real time robot system [4].

5 CONCLUSION AND FUTURE WORKS

This paper proposed a new human-robot interface design method for rehabilitation training of stroke or SCI patients based on sEMG signals. A robust nonlinear model is built to predict the human lower limb movement by using an NARX-DRNN. The sEMG signals and joint angles were collected from five healthy people lower extremity muscles. After preprocessing procedure, three channels of sEMG signals were selected as the inputs of the network by analyzing their correlation with human leg movement. The NARX-DRNN is trained by the Bayesian regularization algorithm which can guarantee its accurate prediction and generation ability. During experiments, two schemes were designed to verify the effectiveness and robustness of the proposed methods. The average joint angles prediction

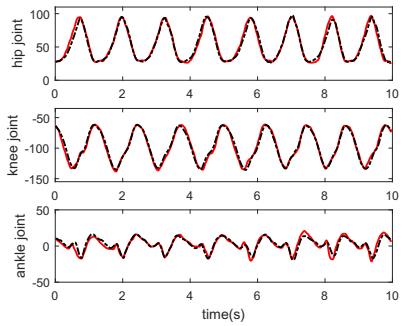

(a) Performance of NARX-DRNN in the subject-independent experiment

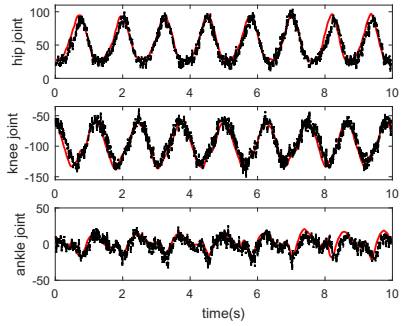

(b) Performance of FFNNAI in the subject-independent experiment

Figure 6: Comparison of the joint angle prediction performance by using NARX-DRNN and FFNNAI in the subject-independent experiment

root-mean-square errors are less than 5° under different experimental schemes. Compared with the traditional FFNNAI model with augmented inputs for motion prediction by using sEMG, the method proposed in this paper improved much in prediction accuracy, robustness and dynamic characteristics. Therefore, the proposed method may supply an effective humanCrobot interface for the robot system. For future works, we are going to popularize this research to stroke patients motion prediction and apply this method to wearable lower limb rehabilitation robots.

6 ACKNOWLEDGEMENTS

This research is supported by the National Natural Science Foundation of China (Grant 61533016, 61203342), Beijing Natural Science Foundation (Grant 4132077) and the Strategic Priority Research Program of the CAS (Grant XDB02080004).

REFERENCES

[1] H. Lee and C. Han, Technical trend of the lower limb exoskeleton system for the performance enhancement, Journal of institute of control, robotics and systems, Vol. 20, No. 3, 364–371, 2014.

[2] A. Villa-Parra, L. Broche, D. Delisle-Rodríguez, R. Sagaró, T. Bastos, and and A. Frizera-Neto, Design of active orthoses for a robotic gait rehabilitation system, Frontiers of Mechanical Engineering, Vol. 10, No. 3, 242–254, 2015.

[3] M. Goldfarb, B. Lawson, and A. Shultz, Realizing the promise of robotic leg prostheses, Science translational medicine, Vol. 5, No. 210, 210–215, 2013.
[4] D. Novak and R. Riener, A survey of sensor fusion methods in wearable robotics, Robotics and Autonomous Systems, Vol. 73, 155–170, 2014.
[5] W. Huo, S. Mohammed, J. C. Moreno, and Y. Amirat, Lower limb wearable robots for assistance and rehabilitation: A state of the art, IEEE Systems Journal, in press, DOI: 10.1109/JSYST.2014.2351491, 2014.
[6] C. Fleischer and G. Hommel, A human–exoskeleton interface utilizing electromyography, IEEE Transactions on Robotics, Vol. 24, No. 4, 872–882, 2008.
[7] F. Zhang, P. Li, Z.-G. Hou, Z. Lu, Y. Chen, Q. Li, and M. Tan, sEMG-based continuous estimation of joint angles of human legs by using bp neural network, Neurocomputing, Vol. 78, No. 1, 139–148, 2012.
[8] R. Gopura, K. Kiguchi, and Y. Li, Sueful-7: A 7DOF upper-limb exoskeleton robot with muscle-model-oriented EMG-based control, in Proceedings of 2009 IEEE International Conference on Intelligent Robots and Systems, 2009: 1126–1131.
[9] R. Song and K. Tong, Using recurrent artificial neural network model to estimate voluntary elbow torque in dynamic situations, Medical and Biological Engineering and Computing, Vol. 43, No. 4, 473–480, 2005.
[10] S. Kwon and J. Kim, Real-time upper limb motion estimation from surface electromyography and joint angular velocities using an artificial neural network for human–machine cooperation, IEEE Transactions on Information Technology in Biomedicine, Vol. 15, No. 4, 522–530, 2011.
[11] J. Ngeo, T. Tamei, and T. Shibata, Continuous estimation of finger joint angles using muscle activation inputs from surface EMG signals, in Proceedings of 34th Annual International Conference of the IEEE Engineering in Medicine and Biology Society, 2012: 2756–2759.
[12] C. Loconsole, S. Dettori, A. Frisoli, C. Avizzano, and M. Bergamasco, An EMG-based approach for on-line predicted torque control in robotic-assisted rehabilitation, in Proceedings of 2014 IEEE Haptics Symposium, 2014: 181–186.
[13] Z. Li, M. Hayashibe, C. Fattal, and D. Guiraud, Muscle fatigue tracking with evoked emg via recurrent neural network: toward personalized neuroprosthetics, IEEE Computational Intelligence Magazine, Vol. 9, No. 2, 38–46, 2014.